Chemical Warfare Simulant-Responsive Polymer Nanocomposites: Synthesis and Evaluation

Sheng-Chun Sha, Rong Zhu, Myles B. Herbert, Julia A. Kalow[1] and Timothy M. Swager *

Department of Chemistry, Massachusetts Institute of Technology, 77 Massachusetts Avenue, Cambridge, MA 02139, United States

[1]Current affiliation: Department of Chemistry, Northwestern University, 2145 Sheridan Rd, Evanston, IL 60208, United States

Correspondence to: T. M. Swager (Email: tswager@mit.edu)

Dedicated to Professor Robert H. Grubbs on the occasion of his 75th birthday

ABSTRACT

Nanomaterials that undergo a physical change upon chemical warfare agent (CWA) exposure can potentially be used in detectors to warn soldiers of their presence or in fabrics to provide on-demand protection. In this study, hybrid nanoparticles (NPs) were prepared by grafting a CWA-responsive polymer from a SiO_2 surface using ring opening metathesis polymerization (ROMP); the covalent functionalization of the polymers on the NP surface was confirmed by GPC, DLS, and TEM analysis. The polymer-grafted SiO_2 NPs were found to undergo a pronounced decrease (ca. 200 nm) in their hydrodynamic radius upon exposure to CWA simulants trifluoroacetic acid (TFA) and diethyl chlorophosphate (DCP) in toluene. This decrease in hydrodynamic radius is attributed to the electrophile-mediated ionization of the triarylmethanol responsive unit, and represents a rare example of polycation formation leading to polymer chain collapse. We have ascribed this ionization-induced collapse to the formation of a favorable stacking interaction between the planar triarylcations. These studies have important implications for the development of breathable fabrics that can provide on-demand protection for soldiers in combat situations.

KEYWORDS: nanocomposites, stimuli-responsive, ROMP, organophosphates, triarylmethanols

INTRODUCTION

The development of polymeric materials that undergo a significant change in macroscopic properties in response to a specific stimulus in a controlled and predictable manner represents a major challenge in materials science.[1] Stimuli-responsive polymers have been widely reported in drug delivery systems, switchable surfaces, and chemical and biological sensors, among other applications.[2] These types of materials undergo structural changes upon exposure to stimuli like heat, light, pH, or solvent addition. In some cases, these structural changes may be translated into a desirable change in physical properties. Systems that respond to tactically relevant analytes in complex military environments, resulting in a targeted macroscopic change, are scarce. We are interested in developing switchable materials that can be implemented into low-cost, robust sensors and protective membranes.

In this context, we have targeted the development of a membrane that displays protective response to a particular class of electrophilic reagents, organophosphate chemical warfare agents (CWAs) (Figure 1a).

This type of material is highly desired for the protection of soldiers in combat settings.[3]

Our strategy involves using a highly breathable, porous surface that is functionalized with a rationally designed responsive polymer (Figure 1b). This polymer would remain extended in the absence of CWAs, leaving the pores open and unobstructed (high breathability, "OFF" state). Reaction with CWAs would cause the polymer chain to collapse and block the pores ("ON" state), such that on-demand protection could be achieved.

Key to the realization of this strategy is the identification of a polymer structure that provides the desired CWA-triggered chain collapse. In contrast, the opposite response is typically observed for polymers reacting with electrophiles. A classical example is the protonation of polyamines, which affords polyammoniums that extend due to charge repulsion (Figure 2a).[4]

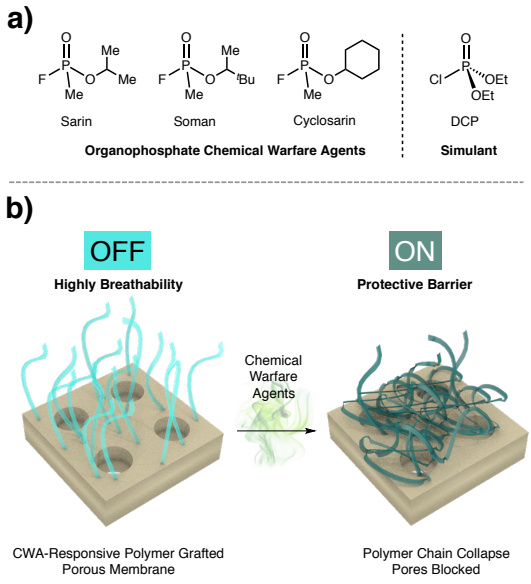

FIGURE 1. a) Chemical structures of common organophosphate CWAs and a less toxic simulant (DCP) used in this study. b) Proposed strategy to achieve a switchable barrier against CWAs. The membrane remains highly breathable in the absence of chemical threats. Upon contact with CWAs, collapsed polymer chains would block the pores and provide protection.

To invert this response, a potential approach is to introduce a responsive unit on the polymer that reacts with electrophiles and generates a delocalized planar cation. We envisioned that the energetically favorable stacking of such cations would cause chain collapse despite the presence of positive charges.[5]

We recently reported triarylmethanol-containing hydrogel polymers that undergo a colorimetric change upon exposure to electrophilic CWA mimics.[6] The response involves CWA-triggered generation of a deep colored trityl cation, which meets the aforementioned requirements for the proposed chain collapse. In fact, it has been observed that in solid state, dimethylamino-substituted trityl cations stack in different patterns with plane distances of as short as 3.3 Å (Figure 2b).[7] Moreover, a preliminary result shows promising volumetric response of the polymer in *bulk* toward trifluoroacetic acid (TFA) vapor.[6] However, this does not guarantee an adequate chain collapsing response in the context of a surface-attached system with relevant polymer length and grafting density.

As a step toward a switchable CWA-protective membrane, our objective is two-fold: (1) identify an efficient method for the covalent surface attachment of the polymers to solid supports and (2) probe the responsive behaviors of polymer chains therein. Due to the limited methods to characterize polymer tethered on a heterogeneous surface, we turned to hybrid nanoparticles as a model system because they can be characterized by solution-phase techniques like dynamic light scattering (DLS), gel permeation chromatography (GPC), and ^{1}H NMR (Figure 2b).

In this study, we have established ring-opening metathesis polymerization (ROMP) as a viable method for grafting diethyl chlorophosphate (DCP)-responsive polymers *from* the surface of SiO_2 nanoparticles (NPs).[8,9] We were able to

observe DCP-triggered polymer chain collapse on these functionalized NPs as indicated by a change in the hydrodynamic volume of the nanocomposite. These results are of crucial importance for the next phase studies of CWA-responsive membranes.

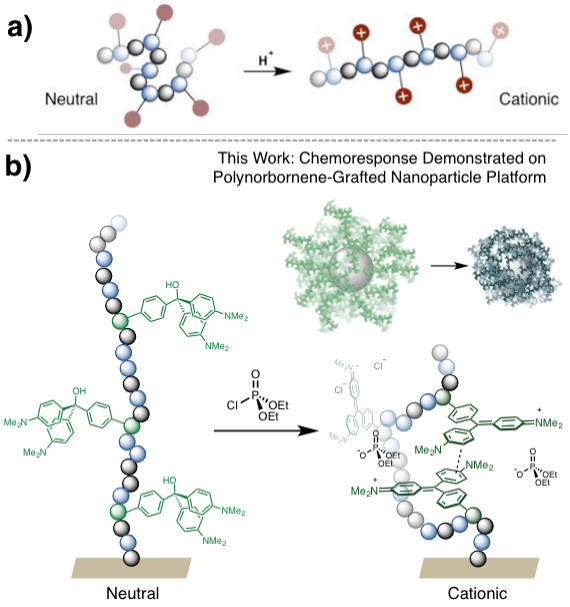

FIGURE 2. a) Electrophiles (e.g. protons) typically trigger polymer chain (e.g. polyamines) extension as a result of the formation of polycation structures. b) Design of triarylmethanol-containing polymers and demonstration of polymer chain collapse upon CWA mimic exposure on a SiO_2 nanoparticle platform (this work).

EXPERIMENTAL

General Methods and Materials

All air- and water-sensitive syntheses were performed in flame-dried flasks under an inert atmosphere with dry argon using standard Schlenk techniques. Tetrahydrofuran, dichloromethane, and toluene were taken from an Innovative Technologies solvent purification system containing activated alumina columns and stored under argon over 3Å or 4Å molecular sieves. Reaction progress was monitored by thin layer chromatography (Merck silica gel 60 F254 plates). ^{1}H (and ^{13}C) NMR spectra were recorded at 400 MHz (100 MHz) using Bruker AVANCE-400. Chemical shifts are reported in ppm and referenced to residual NMR solvent peaks. Gel permeation chromatography (GPC) measurements were performed in tetrahydrofuran using an Agilent 1260 Infinity system and calibrated with polystyrene standards. ATR–FTIR spectra were acquired using a Thermo Scientific Nicolet 6700 FT–IR with a Ge crystal for ATR and subjected to the 'atmospheric suppression' correction in OMNIC™ Specta software. Transmission electron microscopy (TEM) was performed on a FEI Tecnai G2 Spirit TWIN instrument. Dynamic light scattering (DLS) data were obtained on a NanoBrook Omni Particle Size Analyzer and analyzed with Particle Solutions software (version 2.6). Unless otherwise noted, all DLS measurements were performed at ambient temperature (light source: 640 nm, collection angle: 90°). Centrifugation was carried out using Eppendorf centrifuge 5804 with 6 x 85 mL high-speed rotor (F-34-6-38) and Falcon high-performance centrifuge tubes.

All reagents except those noted were used without further purification. Air- or moisture-sensitive reagents were stored under nitrogen using standard Schlenk techniques. Tricyclohexylphosphine (TCP) (97%), ethyl vinyl ether (99%), diethyl chlorophosphate (DCP) and dimethoxymethylphosphonate (DMMP) were purchased from the Sigma Aldrich. Tetraethyl orthosilicate (TEOS) (98%) was purchased from Acros. Triethylamine was distilled over CaH_2 and stored under N_2. Norbornenylethyl triethoxysilane was synthesized from commercially available norbornenylethyl trichlorosilane via one-step ethanolysis.[8a] Grubbs 3rd generation catalyst (**G3**) was prepared from Grubbs 2nd generation catalyst following a literature procedure.[10] Ethyl alcohol (dehydrated 200 proof) was purchased from Pharmco Products Inc., and hydrofluoric acid (HF) (48-50 wt%) and ammonium hydroxide

(28-30 wt%) were purchased from EM Science. DCP was always filtered over K_2CO_3 immediately prior to use, thereby removing any acid impurities that might have formed during storage. Monomers **1**, **2**, **3**, **4** and **5** were synthesized according to literature procedures.[6,11]

WARNING: Diethyl chlorophosphate (DCP), DMMP, and aq. HF are toxic/corrosive hazardous materials and should be treated with great care using appropriate safety measures. Before working with these reagents, one should consult the respective material safety data sheets (MSDS) and other pertinent safety information and understand the risks involved.

Synthesis of Nanoparticles

NP-norbornene. A solution of Stöber silica nanoparticles[9a] (100 mL, 10 mg/mL in ethanol) was stirred with norbornenylethyl triethoxysilane (3 mmol/g SiO_2) overnight at 70 ^oC. An aliquot was removed to determine effective diameter in EtOH. 20 mL PhMe was added and the majority of the EtOH was distilled off at 110 ^oC under atmospheric pressure. The residue was precipitated into hexane. Solids were collected by centrifugation (289 g (1500 rpm); any faster would cause the NPs to irreversibly aggregate). The supernatant was removed and the residue was resuspended in toluene. This sequence was performed 5x total. After the last precipitation, the solids were suspended in 30 mL THF and centrifuged to remove any aggregates. The supernatant was transferred to a graduated cylinder. 1 mL was removed and transferred to a tared vial; the solvent was evaporated carefully to determine the wt% and the volume of the suspension and the graduated cylinder was adjusted with THF to obtain a 20 mg/mL solution. The diameter of the NPs was measured by DLS in THF. The suspension was transferred to a storage flask containing activated 4Å MS and degassed by three freeze-pump-thaw cycles, then transferred to a glovebox.

FT–IR (ATR, v/cm^{-1}): 1078 (s), 951 (m), 798 (m).

General Procedure for SI-ROMP: **NP-P3**. **G3** (10.6 mg, 0.012 mmol) and monomers **5** (4 mg, 0.009 mmol), **4** (7 mg, 0.018 mmol) and **3** (18.6 mg, 0.033 mmol) were weighed in vials outside of the glovebox. A stir bar was placed into the vial containing the **G3**. These were then transferred into the glovebox. Under N_2 atmosphere, the monomers were dissolved in 1 mL THF. **G3** was dissolved in 1 mL **NP-norbornene** stock suspension (20 mg/mL) and stirred for 30 minutes. Next, 0.1 mL of a solution of PCy_3 (0.1 M in THF) was charged to the reaction, which turned brown. Hexanes was added to the reaction until the NPs began to precipitate. At this point the excess catalyst was removed by five cycles of precipitation/trituration. The supernatant was removed and the NPs were resuspended in THF before the each cycle. These cycles were repeated until the supernatant was nearly clear. The NPs were resuspended in 1 mL THF and 0.1 mL of PCy_3 solution was added. This solution was then added to the monomer solution. The reaction was stirred for overnight then removed from the glovebox and quenched with excess ethyl vinyl ether. The nanoparticles were then purified by precipitation into hexane.

FT–IR (ATR, v/cm^{-1}): 2923 (m), 2875 (m), 1741 (s), 1701 (s), 1612 (m), 1519 (m), 1449 (m), 1349 (m), 1093 (s), 967 (m), 816 (m).

Varying polymer shell thickness (Figure 7): Following General Procedure for SI-ROMP with a slight modification, a smaller size NP (242 nm eff. diameter in THF) was obtained using 1 mL CH_2Cl_2 instead of THF as the solvent for the monomers of the same ratio of **NP-P3**. Similarly, a larger size NP (635 nm) was synthesized by doubling the concentrations of the catalyst substituted NP and monomers in THF used in General Procedure for SI-ROMP.

NP-P4. Following General Procedure for SI-ROMP, **NP-P4** was synthesized using 1 mL **NP-norbornene** stock suspension (20 mg/mL), **G3** (10.6 mg, 0.012 mmol) and monomers **4** (11 mg, 0.027 mmol) and **3** (18.6 mg, 0.033 mmol) in 1 mL THF.

NP-P1. Following General Procedure for SI-ROMP with slight modification, catalyst substituted NP was prepared from 2 mL **NP-norbornene** stock suspension (20 mg/mL) and **G3** (21.2 mg, 0.024 mmol) and diluted with THF to a 4 mL suspension. This suspension was divided evenly and each fraction was charged with monomer **1** solution in THF (1 mL) of different concentrations (0.03 M, 0.3 M, 0.6 M, 1.5 M) to afford **NP-P1** of varying sizes.

Dissolving SiO_2 core: In 2-mL plastic centrifuge tubes 5 mg **NP-P1** was dissolved in minimal THF (~0.1 mL). The tube was charged with 0.5 mL aq. HF (48%) and 0.5 mL water. The tube was placed in a plastic bag for added protection and placed on the shaker overnight. The tube was centrifuged and aqueous HF was removed with a plastic syringe. The residue was rinsed 3x with water and 2x with MeOH, dried on high vacuum, and finally dissolved in THF and measured by GPC.

NP-P2. Following General Procedure for SI-ROMP, **NP-P2** was synthesized using 1 mL **NP-norbornene** stock suspension (20 mg/mL), **G3** (10.6 mg, 0.012 mmol) and monomers **2** (30.4 mg, 0.06 mmol) in 1 mL THF.

RESULTS AND DISCUSSION

We commenced our study by synthesizing a SiO_2 NP covalently substituted with N-alkyl substituted **P1** as a model system for evaluating the efficiency and tunability of the polymer grafting reaction (Figure 3a). Norbornene-substituted SiO_2 NP (**NP-norbornene**) was prepared as previously described[8a] and treated with a solution of Grubbs 3rd generation catalyst (**G3**) and PCy_3 to increase the stability of the catalyst-substituted NP. After washing away unreacted ruthenium by repeated precipitations, the NP was taken up in a solution of norbornene-based monomer **1** and polymer **P1** was grafted *from* the NP surface. This SI-ROMP reaction was carried out in THF with different concentrations of monomer **1** (0.03-1.5 M).

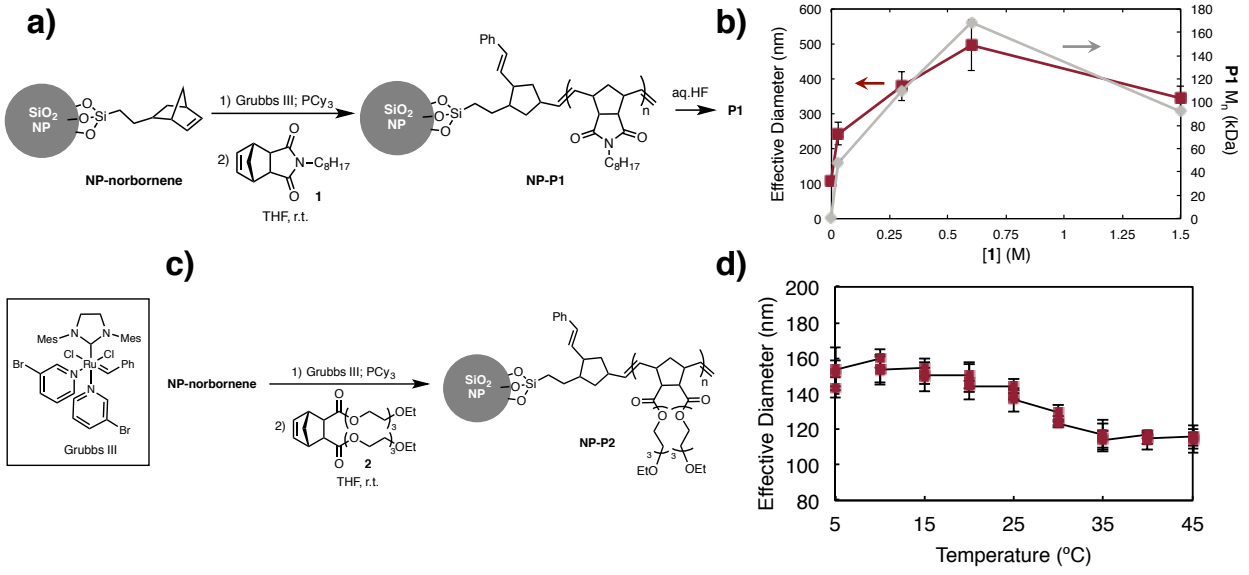

FIGURE 3. a) SI-ROMP synthesis of **NP-P1** with varying monomer **1** concentrations and cleavage of **P1** off the surface. b) Correlation between **NP-P1** particle size (red plot, error bars indicate polydispersity, determined by DLS in THF) and the molecular weight of released polymer **P1** (gray plot, determined by GPC in THF). c) Synthesis of thermo-responsive **NP-P2**. d) Effective diameter of **NP-P2** determined by DLS

in water at varying temperatures. Three independent measurements were conducted. Error bars indicate polydispersity.

It was found that a polymer layer of substantial thickness could be formed even under a dilute monomer concentration (0.03 M, 243 nm) (Figure 3b). The size of the nanocomposite increased with monomer concentration, up until 0.6 M (496 nm), after which it exhibited a slight decrease in hydrodynamic radius.[12]

We then wanted to test if the DLS data of the polymer-substituted NPs matched the GPC data of the corresponding untethered polymers. The nanocomposites were thus treated with HF, leading to dissolution of the SiO_2 NPs and release of the grafted polymers. These free polymers were analyzed by GPC. Gratifyingly, it was found that the number weighted molecular weights (M_n) ranged from 48 to 169 kDa and showed consistent trends when compared to the effective NPs diameter (Figure 3b).

Next, we decided to test the effectiveness of monitoring polymer chain collapse on this nanoparticle platform using a known thermo-responsive polymer **P2**; this material displays a lower critical solution temperature at 25 °C in water. Using the same SI-ROMP protocol as above, **P2** was grafted *from* **NP-norbornene** (Figure 3c). We were able to observe the expected LCST transition by DLS, which exhibited a 40 nm decrease in the particle size upon heating above 25 °C (Figure 3d).

With these results in hand, we set out to investigate nanocomposites functionalized with CWA-responsive polymers (Figure 4). By reacting ruthenium catalyst-substituted NPs with a mixture of monomers **3**, **4**, and **5**, a random copolymer containing a CWA-responsive triarylmethanol unit was grafted *from* **NP-norbornene** to afford **NP-P3**. Incorporation of oligoethylene glycol derived sidechains (**3**) and alkyl groups (**4**) ensured good solubility of the nanocomposites in a range of solvents, even at large particle size. In addition, we also prepared a NP functionalized with a control polymer that lacks the CWA-responsive unit (**NP-P4**).

Effective diameters of **NP-norbornene**, **NP-P3** and **NP-P4** were measured by DLS in THF solutions (Figure 5a). After polymer grafting, the particle sizes increased from 125 nm to 458 nm (**NP-P3**) and 474 nm (**NP-P4**) respectively, indicating the formation of polymer chains of ca. 170 nm in the extended state solvated by THF.

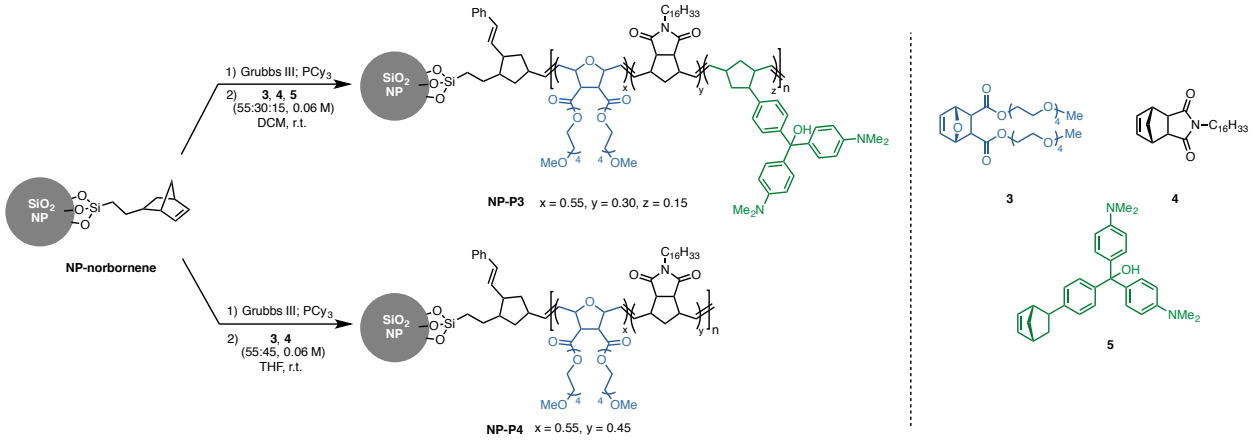

FIGURE 4. Grafting a CWA-responsive polymer and control polymer *from* **NP-norbornene** via ROMP.

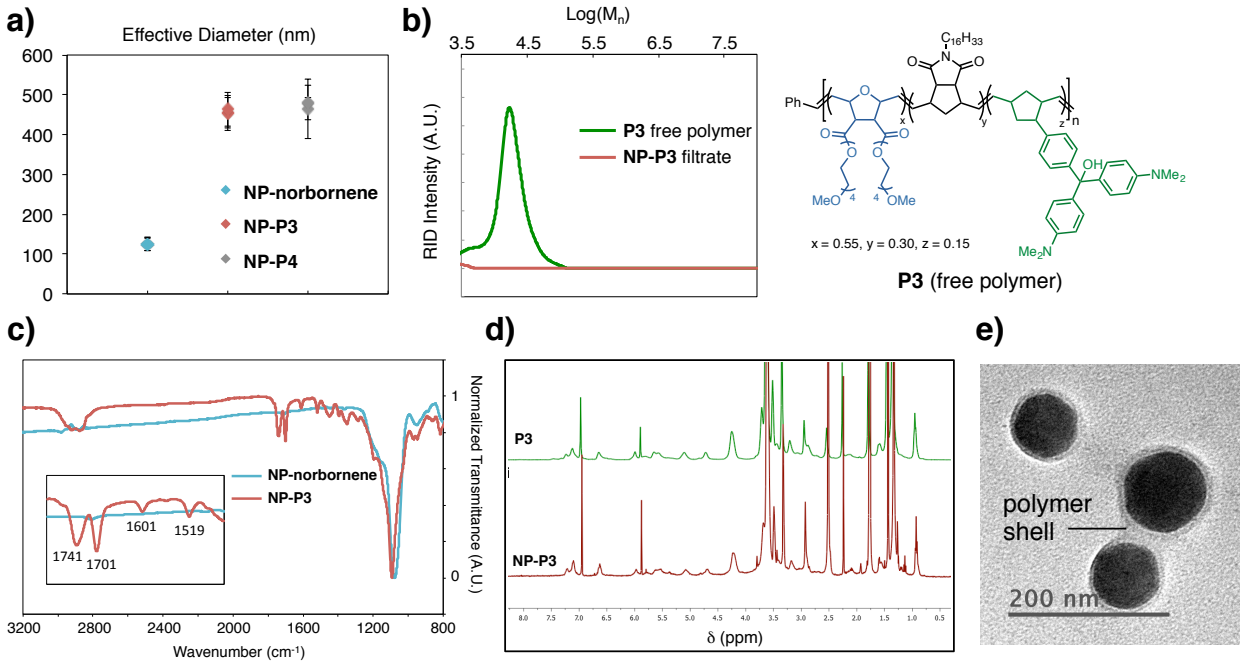

FIGURE 5. Characterization of composites **NP-norbornene**, **NP-P3** and **NP-P4**. a) Effective diameters of **NP-norbornene**, **NP-P3** and **NP-P4** determined by DLS in THF. Three measurements were conducted. Error bar indicate dispersity. b) GPC overlay of free polymer **P3** (green) and a filtrate of **NP-P3** THF solution through a 200 nm PTFE filter (red). c) FTIR spectra overlay of **NP-norbornene** and **NP-P3**. Inset: zoom in from 1450 to 1800 cm^{-1}. d) ^{1}H NMR spectra of free polymer **P3** and **NP-P3** in THF-d_8. e) TEM image of **NP-P3**.

To test the existence of any non-surface attached polymer we filtered a sample of **NP-P3** in THF solution through a 200 nm PTFE filter, and analyzed the filtrate by GPC (Figure 5b). A control sample containing free polymer **P3** prepared under same conditions using homogenous ruthenium catalyst was also filtered and analyzed for comparison. The result suggests that the **NP-P3** sample contained negligible non-tethered polymer.

Next, we compared the FTIR spectra of **NP-norbornene** and **NP-P3** (Figure 5c). After the SI-ROMP step, characteristic bands for ester carbonyl (1741 cm^{-1}), imide carbonyl (1701 cm^{-1}), and triarylmethanol aromatic carbon –carbon bond (1601 and 1519 cm^{-1}) stretches were observed. The incorporation of these functional groups was further confirmed by ^{1}H NMR spectroscopy (Figure 5d, for assignment of the peaks, see Figure S3). Moreover, the spectrum of **NP-P3** was nearly identical to that of free polymer **P3** with the same monomer composition, indicating the randomness of the polymerization process was not affected significantly on a surface. Finally, we were able to directly observe the polymer shell distinct from the inorganic core via transmission electron microscopy (TEM) (Figure 5e). However, due to the vacuum applied, the polymer chains collapsed, preventing further estimation of the shell thickness using TEM.

In order to test our hypothesis that ionization of the triarylmethanol could cause polymer collapse, we first studied the reaction between the nanocomposites and trifluoroacetic acid (TFA), a less toxic reagent that provides fast and complete ionization of triarylmethanol responsive units. For this experiment, we monitored the effective diameters of **NP-P3** and **NP-P4** in THF solution before and after TFA addition using DLS (Figure 6, left panel). It was observed that the presence of TFA had little

effect on the hydrodynamic volume of the control **NP-P4** as expected. For **NP-P3**, particles of smaller size were detected. However, significant particle aggregation occurred upon trityl cation formation, as a significant number of large-diameter particles (>1 μm) were detected by DLS and led to an overall increased average size accompanied by a large polydispersity (>1). This prevented an accurate assess of the behavior of individual NP. Similar observations were made when **NP-P3** was reacted with TFA in the presence of a polar protic solvent such as H_2O, which is known to solvate charged species (Figure 6, middle panel). This aggregation is attributable to strong aromatic interactions between planar trityl cations in these solvents, which could occur both within an individual NP shell, and between multiple NPs. Thus, we hypothesized that performing the ionization in an aromatic solvent would offer appropriate solvation of the trityl cation so that the inter-particle aggregation would be attenuated and intra-shell interactions could be observed.

Thus, we performed the remaining nanocomposite TFA exposure experiments in toluene (Figure 6, right panel). Indeed, after TFA exposure, a substantial decrease in diameter (156 nm) was observed for **NP-P3** under these conditions, which suggests the polymer shell collapsed to nearly 50% of the initial thickness. The polydispersity of **NP-P3** remained unchanged after exposure. As expected, **NP-P4** displayed minimal response.

In addition, we were able to tune the initial polymer shell thickness by simple modifications of the SI-ROMP conditions. Nanocomposites possessing CWA-responsive polymer shells of varying thickness were obtained employing the same monomer combination as was used for **NP-P3**. It was found that the magnitude of the response increased as the thickness of the polymer shell increased (Figure 7). The ability to control the length and collapse magnitude of the polymer grafted would be important for future balancing the membrane's breathability and protective efficiency in different states.

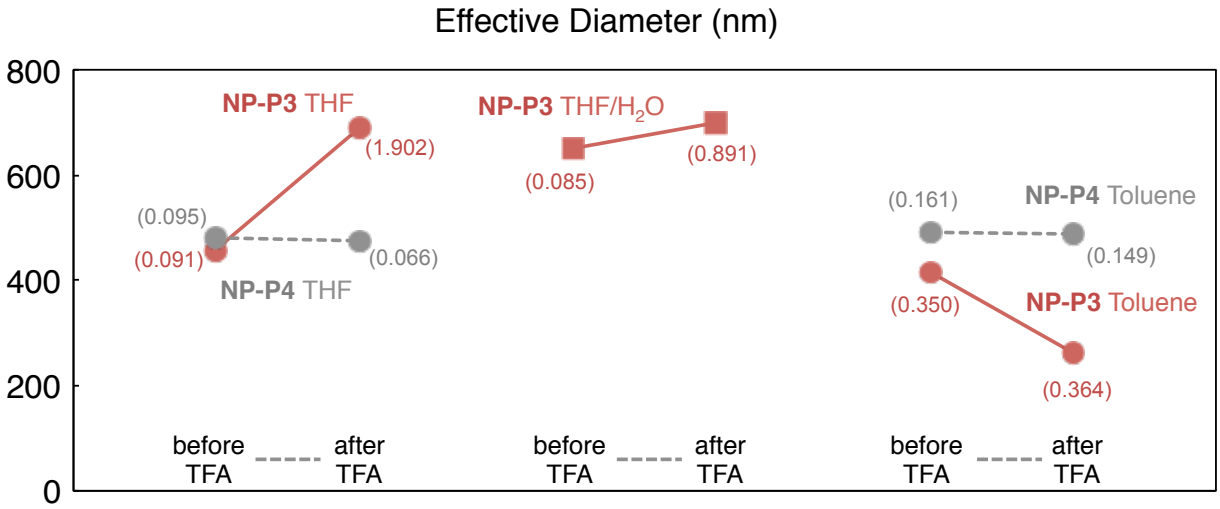

FIGURE 6. Effective diameters of nanocomposites in response to trifluoroacetic acid (TFA) in solution. Red solid: **NP-P3**; grey dash: **NP-P4**. Polydispersity is shown in parentheses.

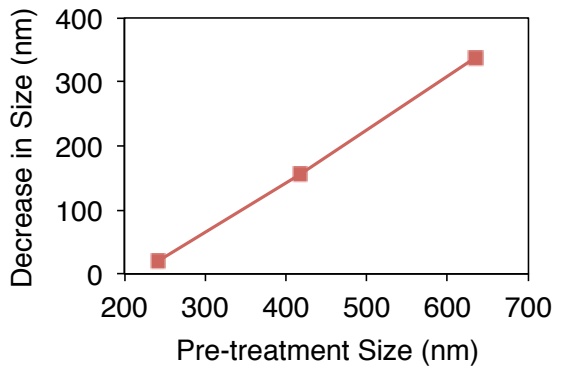

FIGURE 7. Responsive nanocomposites of varying sizes afford different response magnitudes toward TFA exposure.

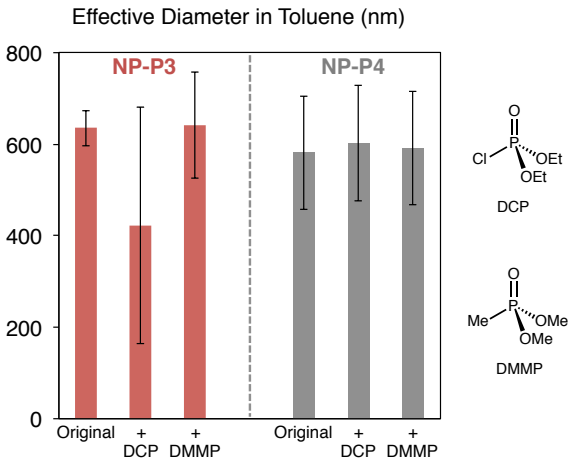

FIGURE 8. Responses of **NP-P3** (red bars) and **NP-P4** (gray bars) towards CWA mimic exposures. Error bars indicate polydispersity.

The most important test is to evaluate whether **NP-P3** responds to established CWA simulants with a similar polymer shell collapse. To this end, we treated **NP-P3** and **NP-P4** with DCP in toluene (Figure 8). Gratifyingly, we observed an over 200 nm decrease in particle size for **NP-P3** while the triarylmethanol-lacking **NP-P4** did not respond. In contrast, dimethoxy methylphosphonate (DMMP), a non-covalent-functionalizing CWA mimic that does not react with the triarylmethanol structure, did not induce an observable response for **NP-P3** or **NP-P4**. This is consistent with our hypothesis that the formation of trityl cations is responsible for the polymer shell collapse.

CONCLUSIONS

In summary, we have synthesized and thoroughly characterized a triarylmethanol-containing responsive ROMP polymer-functionalized SiO_2 nanoparticle. We used this nanocomposite as a platform to demonstrate and characterize CWA simulants-triggered polymer chain collapse. This nanocomposite was found to undergo a pronounced decrease (ca. 200 nm) in its hydrodynamic radium upon exposure to the TFA and CWA simulant DCP in toluene. We propose that the electrophile-mediated ionization of the triarylmethanol responsive unit is responsible for the polymer collapse via stacking of planar cations. This represents a rare example where formation of polycations affords polymer chain collapse. These studies have important implications for the development of breathable fabrics that can provide on-demand protection for soldiers in combat situations.

ACKNOWLEDGEMENTS

The authors would like to acknowledge the financial support of the Chemical and Biological Technologies Department at the Defense Threat Reduction Agency (DTRA–CB) via Contract BA12PHM123 in the "Dynamic Multifunctional Materials for a Second Skin D[MS]^{2}" program. M.B.H. is supported by a F32 Ruth L. Kirschtein NRSA Postdoctoral Fellowship. The authors would like to thank Dr. F. Fornasiero (Lawrence Livermore National Laboratory, CA) and Prof. J. Shan (Rutgers University) for insightful discussion, and I. Jeon (MIT) for conducting TEM imaging experiments.

REFERENCES AND NOTES

1. (a) Wei, M.; Gao, Y.; Li, X.; Serpe, M. J. *Poly. Chem*. **2017**, *8*, 127-143. (b) Motornov, M.; Roiter, Y.; Tokarev, I.; Minko, S. *Prog. Polym. Sci*. **2010**, *35*, 174-211. (c) Manna, A.; Chen, P.-L.; Akiyama, H.; Wei, T.-X.;

Tamada, K.; Knoll, W. *Chem. Mater*. **2003**, *15*, 20-28. (d) Tang, Z.; Lim, C.-K.; Palafox-Hernandez, J. P.; Drew, K. L. M.; Li, Y.; Swihart, M. T.; Prasad, P. N.; Walsh, T. R.; Knecht, M. R. *Nanoscale* **2015**, *7*, 13638-13645.

2. Stuart, M. A. C.; Huck, W. T. S.; Genzer, J.; Muller, M.; Ober, C.; Stamm, M.; Sukorukov, G. B.; Szleifer, I.; Tsukruk, V. V.; urban, M.; Winnik, F.; Zauscher, S.; Luzinov, I.; Minko, S. *Nature Mater*. **2010**, *9*, 101-113.
3. (a) Boopathi, M.; Singh, B.; Vijayaraghavan, R. *The Open Textile Journal* **2008**, *1*, 1-8. (b) Bui, N.; Meshot, E. R.; Kim, S.; Peña, J.; Gibson, P. W.; Wu, K. J.; Fornasiero, F. *Adv. Mater.* **2016**, *28*, 5871-5877. (c) Martin, B. D.; Justin, G. A.; Moore, M. H.; Naciri, J.; Mazure, T.; Melde, B. J.; Stroud, R. M.; Ratna, B. *Adv. Funct. Mater.* **2012**, *22*, 3116-3127.
4. Huck, W. T. *Materials Today*, **2008**, *11*, 24-32.
5. Martinez, C. R.; Iverson, B. L. *Chem. Sci.*, **2012, *3*,** 2191-2201
6. (a) Lovell, S.; Marquardt, B. J.; Kahr, B.; *J. Chem. Soc., Perkin Trans. 2*, **1999**, 2241-2247. (b) Guo, S. X.; Xie, J.; Gilbert-Wilson, R.; Birkett, S. L.; Bond, A. M.; Wedd, A. G. *Dalton Trans.*, **2011**, *40*, 356-366.
7. Belger, C.; Weis, J. G.; Egap, E.; Swager, T. M. *Macromolecules* **2015**, *48*, 7990-7994.
8. (a) Jordi, M. A.; Seery, T. A. P. *J. Am. Chem. Soc*. **2005**, *127*, 4416-4422. (b) Radhakrishnan, B.; Ranjan, R.; Brittain, W. J. *Soft Matter* **2006**, *2*, 386-396.
9. (a) Weck, M.; Jackiw, J. J.; Rossi, R. R.; Weiss, P. S.; Grubbs, R. H. *J. Am. Chem. Soc*. **1999**, *121*, 4088-4089. (b) Kim, N. Y.; Jeon, N. L.; Choi, I. S.; Takami, S.; Harada, Y.; Finnie, K. R.; Girolami, G. S.; Nuzzo, R. G.; Whitesides, G. M.; Laibinis, P. E. *Macromolecules* **2000**, *33*, 2793-2795. (c) Moon, J. H.; Swager, T. M. *Macromolecules* **2002**, *35*, 6086-6089. (d) Liu, Y.; Adronov, A. *Macromolecules* **2004**, *37*, 4755-4760. (e) Jiang, G.; Ponnapati, R.; Pernites, R.; Felipe, M. J.; Advincula, R. *Macromolecules* **2010**, *43*, 10262-10274. (f) Carlsson, L.; Malmström, E.; Carlmark, A. *Polym. Chem*. **2012**, *3*, 727-733.
10. (a) Love, J. A.; Morgan, J. P.; Trnka, T. M.; Grubbs, R. H. *Angew. Chemi. Int. Ed*. **2002**, *41*, 4035-4037. (b) Choi, T.-L.; Grubbs, R. H. *Angew. Chem. Int. Ed*. **2003**, *42*, 1743-1746.
11. Bauer, T.; Slugovc, C. *J. Polym. Sci., Part A: Polym. Chem.* **2010**, 48, 2098– 2108.
12. At very high monomer concentrations unfavorable medium effect could occur and lead to decrease in chain length.

GRAPHICAL ABSTRACT

Sheng-Chun Sha, Rong Zhu, Myles B. Herbert, Julia A. Kalow and Timothy M. Swager*

Chemical Warfare Simulant-Responsive Polymer Nanocomposites: Synthesis and Evaluation

Chemical warfare agents continue to post a threat to civilians and military personnel in conflict zones. As a step toward a breathable hybrid fabric that provides on-demand protection against these agents, we have synthesized a triarylmethanol-containing responsive polymer-substituted nanoparticle using surface-initiated ring-opening metathesis polymerization. Using this nanocomposite as a platform we have demonstrated tunable chain collapsing response upon exposure to agent simulants, which is the key to the proposed protecting scheme.